A New Deep Learning-Based Restoration Method for Colour Images

Songshan Zu

Department of Environmental Design, Academy of Fine Arts, Changchun University, Changchun 130000, China

Corresponding Author Email: zuss@ccu.edu.cn

ABSTRACT

As color images have been widely used in many fields, their restoration problem has received wide attention from researchers. This study proposed two solutions for denoising and low illuminance enhancement problems of existing color image restoration methods. At first, this paper built a colour image denoising model of weighted Schatten-p norm based on deep learning, which fully considers differences in the noise level of each channel of colour images, and could give a better denoising effect. Then, this study proposed a low illuminance color image enhancement algorithm that combines Gamma transform and Contrast Limited Adaptive Histogram Equalization (CLAHE), which could better balance image contrast enhancement and noise suppression. Studies of these two parts have both gained good results in terms of theory and experiment, and they could push the progress of colour image restoration technology and provide valuable references for related fields.

1. INTRODUCTION

Images could be found in every corner of people's lives as they are an important carrier in this modern digital world. Especially the color images have been widely used in various fields including social media, medical diagnosis, distance education, commercial advertisement, and security monitoring due to their rich color information and excellent visual performance [1-4]. However, affected by factors such as camera equipment, transmission process and storage devices, colour images are often subject to noise pollution during acquisition, transmission and processing, which can adversely affect their visual quality and value in practical applications [5, 6]. Besides, in low illumination environments, the clarity and contrast of color images would decline dramatically due to insufficient light, which can hurt their visibility and practicality. Therefore, colour image restoration, especially denoising and low illumination enhancement, are important topics in the research field of image processing [7-9].

Research on colour image restoration is not only of great value for enhancing visual effect and quality of images, but also important for many practical application scenarios, for instance, in remote sensing imaging, image quality can directly affect the recognition and classification of surface features [10-12]; in medical imaging, image quality is closely related to the accurate diagnosis of diseases [13-15]; in security monitoring and automatic driving, image quality determines the accuracy of target detection and tracking [16-19]. Therefore, the research on colour image restoration is of utterly importance for the application of images in various fields.

Now the study of modern art design is not only limited to painting and design skills in the traditional way, with the advancement of science and technology, computer graphics, image processing, and other computer-aided design techniques have been extensively used in modern art design

[20, 21]. In this context, the research on colour image restoration methods is particularly important for the study of art design, as designers often need to complete their design works by using or modifying high-quality images. If the original images contain noises or blurs, the image restoration methods can be adopted to improve the quality of these images [22-25]. Besides, the research on colour image restoration methods can help students deepen their understandings about the use of colors, and get a more accurate mastery of grey scale, contrast, color balance and other aspects of images, and these can inspire students to generate more creative ideas, and provide them with more skills and tools when designing their works.

However, despite the fact that many researchers have conducted in-depth studies on colour image restoration methods, there are shortcomings with existing methods and challenges pending for solution. For one thing, the difference in noise levels of each channel of color images hasn't been fully considered in currently available denoising models, which often results in unbalanced denoising effect of each channel during practical operations, thereby adversely affecting visual effect and information extraction. For anther thing, for low illumination colour images, the existing enhancement methods can hardly find a good balance between image contrast enhancement and noise suppression, so the enhancement effect of these methods often fails to meet actual needs.

In view of these matters, in this work, a colour image denoising model of weighted *Schatten-p* norm was constructed based on deep learning, the model fully considers the difference in noise levels of each channel of colour images, and could give a better denoising effect. Then, a low illuminance color image enhancement algorithm that combines *Gamma* transform and *CLAHE* algorithm was proposed, aiming at finding a good balance between image contrast enhancement and noise suppression. Through these

works, we hope to further advance the development of colour image restoration techniques and provide useful evidences for research and applications in related fields.

2. THE IMPROVED COLOUR IMAGE DENOISING MODEL

Colour image restoration is an important topic in image processing, and its goal is to restore the damaged color images and generate clearer images. During the restoration process of color images, denoising and enhancement are two key links.

Denoising is the first and most critical step in color image restoration. During the actual image acquisition, transmission and storage processes, due to the influence of various factors, such as equipment noise, communication noise, and compression distortion, images are often subject to noise pollution, and these noises can hurt image quality, reduce visual effect, even cause information loss. Therefore, denoising is an essential step in the restoration process, and its goal is to remove noise from images while retaining image details and edge information as much as possible, thereby generating clear, noise-free images.

Colour image enhancement is another important step in color image restoration, and its goal is to enhance the visual effect of images, making them more suitable for subsequent analysis and processing. Especially for color images captured under low illumination or poor lighting conditions, due to insufficient ambient light, the contrast and brightness of images will be both reduced, resulting in low image clarity and visibility. Through image enhancement, the brightness and contrast of these images can be improved, image details and features can be highlighted, which is conductive to subsequent image analysis and processing.

A colour image is a three-dimensional data structure, unlike the two-dimensional matrix of grey-scale image, if we simply slice a high-dimensional colour image, reduce it to a number of two-dimensional matrices and process it using two-dimensional denoising algorithms (such as the *WSNM*), then the internal structure of the image might be damaged, and the self-similarity of the image in the third dimension (such as colour channels) might be ignored. Moreover, in colour images, different colour channels may contain noises of different levels. If we deal with the noises of each channel separately without considering the difference between them, then artefact might be generated in the denoised images. In view of these problems, this paper proposed a deep learning model based on weighted *Schatten-p* norm, which fully considers the difference in the noise level of each channel of color images, learns and utilizes the complex features and patterns of image data, thereby effectively removing the noise.

For a given noise-containing color image, a local block sized o*o*3 was taken from each channel, and each local block was stretched to generate a tile vector $t=[t^Y_E, t^Y_H, t^Y_N] \in R^{3O2}$, wherein $t_E, t_H, t_N \in E^{o2}$ respectively correspond to three channels R,G,B; for each t, a search box was set, within each box, L similar blocks were found for each channel, and all blocks were stacked. Assuming: Z and B represent denoised matrix and noise matrix, then through above steps, a noise-containing block matrix was generated and represented by $T=Z+B \in E^{3o2*}$.

In the standard R,G,B space, the noise can be approximated simulated as additive Gaussian white noise, but the noise variance of different channels may differ as well. If this difference is ignored and a uniform denoising method is directly used, then it may not be able to achieve the best denoising effect. To solve the different noise intensities existing in different channels of colour image, this paper introduced a weighting matrix, which assigns a weight to each channel to realize flexible processing based on the noise intensity of each channel, thereby making the denoising process be more in line with the actual situation. Figure 1 shows the principle of the constructed denoising model.

On this basis, a multichannel double-weighted *Schatten-p* norm minimization denoising model was proposed. Assuming: $\gamma>0$ is a very small value; $\delta_u(Z_j)$ represents the u-th singular value of matrix Z after the j-th iteration; $\Psi_1^{j+1}=V/(|\delta^{1/O}_u(Z_j)|+\gamma)$ represents the weight vector Ψ under *Schatten-p* norm.

$$\underset{Z}{MIN} \| \Psi(T-Z) \|^2_D + \| Z \|^o_{Q,A_o} \tag{1}$$

Defining: $T=[T^Y_e, T^Y_h, T^Y_n]$ represents the noise block matrix; T^Y_e, T^Y_h, T^Y_n represent similar block matrices within the three channels; $Z =[Z^Y_e, Z^Y_h, Z^Y_n]$ represents the denoised matrix; Z^Y_e, Z^Y_h, and Z^Y_n are self-similar, then in the framework of maximum a posteriori estimation, Ψ can be estimated as:

$$\hat{Z} = \underset{Z}{\Gamma} \ln O(Z \,|\, T, \Psi) = \underset{Z}{\Gamma} \{ \ln O(T \,|\, Z) + \ln O(T \,|\, Z) \} \tag{2}$$

Features of the noise statistic can be represented by the log-likelihood term $ln\ O(T|Z)$. Assuming: noises in the three channels of R,G,B are independent, identically distributed, and conform to the Gaussian distribution and standard deviation $\{\delta_e, \delta_h, \delta_n\}$, so there is:

$$O(Z \,|\, \Psi) \propto \exp\left(-\frac{1}{2} \| Z \|^o_{Q,A_o} \right) \tag{3}$$

Combining above three formulas, we have:

$$\begin{aligned}
\hat{Z} &= \underset{Z}{\Gamma} \sum_{v \in \{e,g,n\}} \frac{1}{\delta^2_v} \| T_v - Z_v \|^2_D + \| Z \|^o_{Q,A_o} \\
&= \underset{Z}{\Gamma} \| \Psi(T-Z) \|^2_D + \| Z \|^o_{Q,A_o}
\end{aligned} \tag{4}$$

Image with noise   Downsampling images and noise level images   Nonlinear mapping (convolution, block normalization, etc.)   Denoised downsampling image   Denoised image
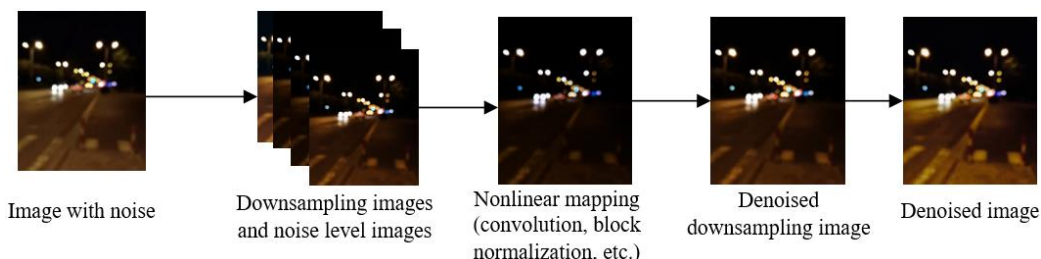
Figure 1. Principle of the constructed denoising model

Assuming: U represents the unit matrix, then there is:

$$\Psi = \begin{bmatrix} \delta_e^{-1}U & 0 & 0 \\ 0 & \delta_h^{-1}U & 0 \\ 0 & 0 & \delta_n^{-1}U \end{bmatrix} \qquad (5)$$

According to above inference, it is known that the weight matrix is a diagonal matrix that can be defined by the standard deviation of noise within each channel, and this means that channels with higher noise intensity will be assigned with larger weights when estimating the denoised matrix Z; on the contrary, channels with lower noise intensity will be assigned with smaller weights. This adaptive weight assignment strategy can more accurately reflect the difference in noise intensity of each channel, thereby improving the denoising effect. The recovery of low-rank structure is an important link in colour image denoising. The proposed model takes the *Schatten-p* norm as the low-rank penalty term, which is more flexible than nuclear norm in solving low-rank problems. When $p=1$, the *Schatten-p* norm degenerates to the nuclear norm, indicating that the proposed model can make use of the advantages of nuclear norm under certain conditions, so the proposed model considers the noise intensity of different channels and uses a flexible low-rank processing method to process multiple channels, thereby achieving good denoising effect with high efficiency.

3. AN IMPROVED LOW ILLUMINANCE COLOUR IMAGE ENHANCEMENT ALGORITHM

Although the conventional Histogram Equalization (*HE*) algorithm is simple and effective, it ignores local features of images when enhancing low illuminance color images, which may lead to over-enhancement or over-suppression of some image regions, and thus affecting the overall visual effect of the image. Besides, for some color images with complex changes in illuminance, the *HE* algorithm may not be able to get the desired enhancement effect. So this study combined the *Gamma* transform with *CLAHE* (Contrast Limited Adaptive Histogram Equalization) algorithm, the combined method uses *Gamma* transform to change the overall brightness of the image and uses *CLAHE* algorithm to improve local contrast. Figure 2 gives a diagram showing the flow of the proposed enhancement algorithm.

Gamma transform is a non-linear grey scale transformation method. Assuming: v represents constant, ε represents correction parameter, then the formula of *Gamma* transform is:

$$a = XH^\varepsilon \quad \varepsilon \in [0,1] \qquad (6)$$

In all cases, v satisfies $v=1$ and the input and output grey levels are represented by e and a:

$$a = v(e+\gamma)^\varepsilon \qquad (7)$$

Enhancement of image regions with different grey levels can be achieved by adjusting the value of correction parameter ε. When $\varepsilon=1$, the transformation is linear, namely there is a proportional relationship between the input grey value and the output grey value, and the overall brightness of the image won't change. When $\varepsilon<1$, the corresponding curve will expand

in low grey level regions, which means that the change of low grey value is greater than the change of high grey value, and this will lead to an enhancement of image details in dark regions. In other words, a value of ε less than 1 will lead to brightness enhancement in dark regions, so details in these regions will be easier to see. When $\varepsilon>1$, the curve will expand in high grey level regions, which means that the change of high grey value is greater than the change of low grey value, and this will lead to an enhancement of image details in bright regions. A value of ε greater than 1 will lead to brightness enhancement in bright regions, so details in these regions will be easier to see.
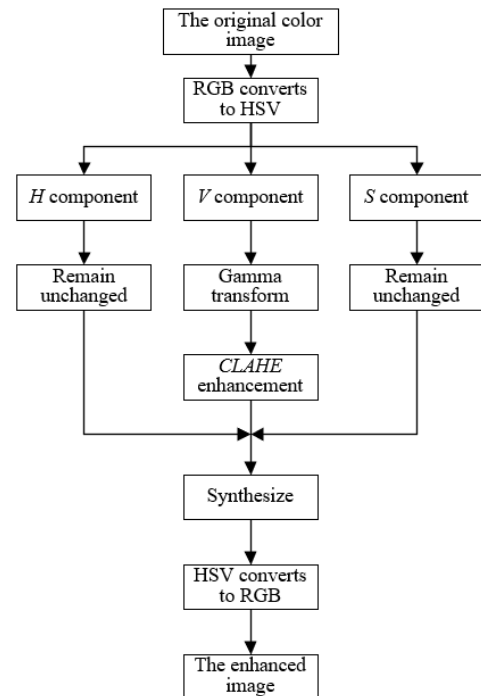

Figure 2. Flow of the enhancement algorithm

The conventional *HE* algorithm stretches the histogram of image, which can improve the contrast of image on the whole, but its enhancement effect in local regions is limited, especially in case of uniformly distributed pixel values. The Adaptive Histogram Equalization (*AHE*) algorithm calculates each local region separately and applies histogram equalization, but it may over-enhance the noise, resulting in image quality decline. To solve this problem, this paper introduced the *CLAHE* algorithm to perform histogram equalization to better enhance the local contrast and brightness of image, and improve its visual effect. Besides, a contrast limit was introduced at the same time to effectively suppress the over-amplification of noise and improve the overall quality of the image.

Steps of algorithm implementation are:

Step 1: Segment image sub-blocks. The image is segmented into smaller sub-blocks to better process local features; this is because in a large image, the brightness and contrast of local regions may be different from the global image, so if the entire image is subjected to histogram equalization, these local changes might be overlooked, resulting in poor processing effect.

Step 2: Count the grey level histogram. The grey level histogram counts the pixel numbers of each grey level in the image, and it provides the base data for subsequent equalization operations.

Step 3: Make the grey levels in image sub-blocks have equal number of pixels: this is the core step of histogram equalization, its aim is to turn grey value distribution into a uniform distribution, thereby enhancing the contrast of the image. Assuming: i_z represents the pixel number of sub-blocks in the horizontal direction; i_t represents the pixel number in the vertical direction; M_{GR} represents the number of grey levels in the sub-block; then the average number of pixels B_{av} can be calculated by the following formula:

$$B_{AV} = \frac{(i_z \times i_t)}{M_{GR}} \tag{8}$$

Step 4: Introduce clipping limit coefficient. This coefficient is used to control the intensity of equalization. If no limit is applied, histogram equalization may result in too-high contrast of some regions, thereby causing image distortion. By setting a clipping limit, the natural feeling of the image can be kept while avoiding the problem of over-enhancement. Assuming: α represents the clipping limit coefficient and its range is [0,1], then the actual clipping limit value B_{SJ} can be calculated by the following formula:

$$B_{SJ} B_{AV} + \left[\alpha \times (i_z \times i_t - B_{AV}) \right] \tag{9}$$

Step 5: Solve the number of pixels assigned to each grey level. Purpose of this step is to achieve uniform distribution as much as possible under the constraint of clipping limit. This clipping limit ensures that the number of pixels of each grey level won't be too much, and the pixels exceeding the limit will be assigned to other grey levels to achieve the effect of equalization. Assuming: B_{CL} represents the total number of clipped pixels, then the number of pixels assigned to each grey level B_{AC} can be solved by the following formula:

$$B_{AC} = \frac{B_{CL}}{M_{GR}} \tag{10}$$

where,

$$B_{CL} = \sum_u \{MAX[G(u) - B_{SJ}, 0]\} \tag{11}$$

Assuming: $G'(u)$ represents the newly attained local histogram after pixel assignment, then its expression is:

$$G'(u) = \begin{cases} B_{SJ}, G(u) > B_{SJ} \\ B_{SJ}, G(u) + B_{AC} \geq B_{SJ} \\ G(u), others \end{cases} \tag{12}$$

The expression of B_{CL} after clipping is:

$$B_{CL} = \begin{cases} B_{CL}, G(u) > B_{SJ} \\ B_{CL} - (B_{SJ} - G(u)), G(u) + B_{AC} \geq B_{SJ} \\ B_{CL} - B_{AC}, others \end{cases} \tag{13}$$

If there are remaining pixels that have not been assigned, then cyclic assignment needs to be carried out, during which these remaining pixels need to be uniformly assigned to grey levels smaller than clipping limit $N_{CL}B_{SJ}$ until all of them have been assigned.

Step 6: Equalization processing. Based on previous processing results, this step adjusts the grey value of each pixel to achieve the effect of contrast enhancement.
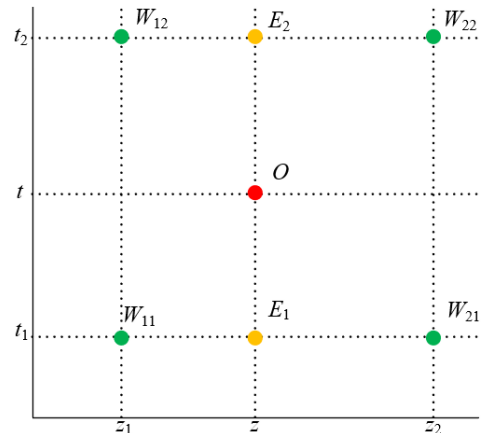

Figure 3. Principle of bi-linear interpolation

Step 7: Use the bi-linear interpolation method to solve new grey values. Sine the image has been segmented into multiple sub-blocks, the processing of each sub-block can result in discontinuities in the boundaries between sub-blocks, thereby generating an obvious block effect. Through bi-linear interpolation, the value of intermediate pixels can be estimated based on the values of four neighbour pixels, thereby realizing smooth transition and mitigating or eliminating the block effect. Figure 3 shows the principle of bi-linear interpolation.
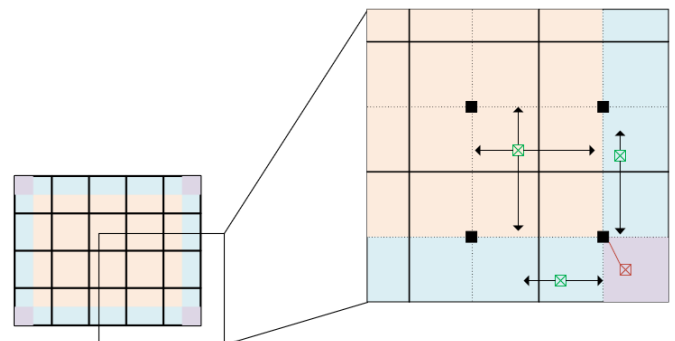

Figure 4. Image segmentation

Figure 4 gives a diagram showing the principle of image segmentation. In the bi-linear interpolation method, set a function d, to calculate its value at point $O(z,t)$ based on the given values of d at four points $W_{11}(z_1,t_1)$, $W_{12}(z_1,t_2)$, $W_{21}(z_2,t_1)$, and $W_{22}(z_2,t_2)$, the linear interpolation was performed once in direction z, then there are:

$$d(E_1) \approx \frac{z_2 - z}{z_2 - z_1} d(W_{11}) + \frac{z - z_1}{z_2 - z_1} d(W_{21}) \tag{14}$$

$$d(E_2) \approx \frac{z_2 - z}{z_2 - z_1} d(W_{12}) + \frac{z - z_1}{z_2 - z_1} d(W_{22}) \tag{15}$$

Similarly, linear interpolation was performed once in direction t, then there is:

$$d(O) \approx \frac{t_2 - t}{t_2 - t_1} d(E_1) + \frac{t - t_1}{t_2 - t_1} d(E_2) \qquad (16)$$

Through above steps, $d(z,t)$ was solved:

$$d(z,t) \approx \frac{d(W_{11})}{(z_2 - z_1)(t_2 - t_1)}(z_2 - z)(t_2 - t)$$
$$+ \frac{d(W_{21})}{(z_2 - z_1)(t_2 - t_1)}(z - z_1)(t_2 - t)$$
$$+ \frac{d(W_{12})}{(z_2 - z_1)(t_2 - t_1)}(z_2 - z)(t - t_1) \qquad (17)$$
$$+ \frac{d(W_{22})}{(z_2 - z_1)(t_2 - t_1)}(z - z_1)(t - t_1)$$

4. EXPERIMENTAL RESULTS AND ANALYSIS

According to Tables 1, 2 and 3, in cases of sparse noise of different levels, the proposed denoising model can accurately restore the rank of images, exhibiting its ability to accurate control the image rank. For low-level sparse noise, the model performed excellently, the relative error was extremely low, the peak signal-to-noise ratio was high, and the structural similarity was close to 1, indicating that the restored image was highly similar to the original image and they were almost indistinguishable. For medium-level sparse noise, although the model was still able to restore the rank accurately, the relative error increased, and the peak signal-to-noise ratio and the structural similarity both decreased, indicating that there were certain differences between the restored image and the original image, but the overall restoration effect was still good. For high-level sparse noise, the model could accurately restore the rank, but the relative error increased, the peak signal-to-noise ratio and the structural similarity decreased, showing a decline in the restoration effect compared with that in cases of low and medium level noise. The improved colour image denoising model proposed in this paper performed excellently in cases of low and medium level noise; as for high level noise, although the restoration effect declined a bit, overall speaking, its denoising ability was good, suggesting that this model is robust to noise of different levels, and it has important practical application value for colour image denoising.
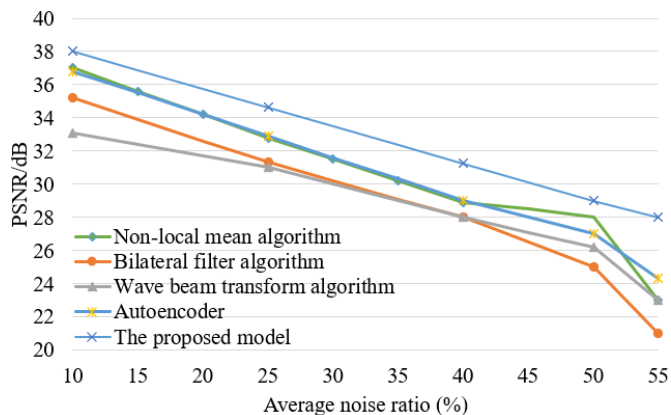

Figure 5. PSNR value of different methods in case of original image added with different-ratio Gaussian noise

According to data shown in Figure 5, it can be known that under each noise level, the proposed model attained higher *PSNR* values than the non-local mean algorithm, the bilateral filter algorithm, the wave beam transform algorithm, and the auto-encoder algorithm, indicating that its denoising effect outperformed the other methods. For the non-local mean algorithm and the auto-encoder, their *PSNR* values declined gradually with the increase of noise ratio, and the decrement was large. This is because the two algorithms showed poor performance when processing Gaussian noise, and they could not remove the noise effectively. The *PSNR* values of the bilateral filtering algorithm and the wave beam transform algorithm also decreased with the increase of noise ratio, but the decrease speed was slow, especially the wave beam transform algorithm, its *PSNR* was high even in case of a noise ratio reaching as high as 55%. This is because the two algorithms were robust when processing the Gaussian noise. Under the condition of increased noise ratio, the decrement of *PSNR* value of the proposed model was the smallest among all algorithms, exhibiting good stability and robustness. And this is due to the fact that the influence of noise had been fully considered during the design of the proposed model and corresponding strategies were adopted to suppress the influence of noise.

Table 1. Color image restoration results in case of low-level sparse noise

Dimension	Rank	Rank of Restored Image	Relative Error	PSNR/dB	SSIM
100	10	10	1.3518e-6	37.21	0.96
200	20	20	1.9762e-6	37.09	0.97
300	30	30	2.4334e-6	36.89	0.96

Table 2. Color image restoration results in case of medium-level sparse noise

Dimension	Rank	Rank of Restored Image	Relative Error	PSNR/dB	SSIM
100	10	10	3.8618e-8	32.96	0.93
200	20	20	4.3212e-8	31.90	0.92
300	30	30	4.3123e-8	30.78	0.91

Table 3. Color image restoration results in case of high-level sparse noise

Dimension	Rank	Rank of Restored Image	Relative Error	PSNR/dB	SSIM
100	10	10	8.9022e-3	26.32	0.71
200	20	20	1.5267e-3	25.96	0.77
300	30	30	1.6728e-3	23.34	0.66

The structural similarity index measure (*SSIM*) is a metric used to measure image quality, and it mainly focuses on the structural information of images. A *SSIM* value closer to 1 indicates that the structural information of the image is retained more completely, and the image quality is better. According to the data in Table 4, on all noise ratios, the proposed model outperformed other methods in terms of the *SSIM* value, indicating that the proposed model had a better performance in retaining the structural information of images. The *SSIM* values of the non-local mean algorithm, the bilateral filtering algorithm, and the wave beam transform algorithm all decreased with the increase of noise ratio, and their decline trends were obvious, indicating that these algorithms had lost some structural information of images during the denoising process. The *SSIM* value of the proposed model also decreased with the increase of noise ratio, but its decrease speed was much lower than that of other algorithms, indicating that the proposed model could better retain the structural information of images during the denoising process, and it was more robust to the noise. Therefore, under all levels of noise, the proposed model can achieve a better denoising effect than other methods, it can better retain the structural information of images, and have higher stability and robustness.

In image processing, mean square error (*MSE*), peak signal-to-noise ratio (*PSNR*), and computation time are commonly used evaluation indicators of algorithms. A smaller *MSE* value indicates less image error and better image quality; a greater *PSNR* value indicates larger signal-to-noise ratio and better image quality; the computation time reflects the efficiency of the algorithm. According to Table 5, it can be concluded that the proposed algorithm had smaller errors in image enhancement. In terms of *PSNR*, it also outperformed the Laplace sharpening algorithm and the multi-scale retina enhancement algorithm, indicating that it can better retain the quality of images in the aspect of signal-to-noise ratio. In terms of computation time, although the proposed algorithm was slower than the other two algorithms, in view of its obvious advantages in *MSE* and *PSNR*, the sacrifice of time is worthwhile. So on the whole, although the proposed algorithm had a slight disadvantage in computation time, it was significantly better than the other two algorithms in terms of

retaining image quality and controlling errors. This also indicates that the proposed enhancement algorithm had high image enhancement performance and can effectively improve image quality.

Figure 6 shows the results of the comparative experiment of color image enhancement. According to the figure, during the image enhancement practice, although the *HE* algorithm, the Laplace sharpening algorithm, and the multi-scale retina enhancement algorithm performed good, the proposed algorithm gave a better effect during the experiment.
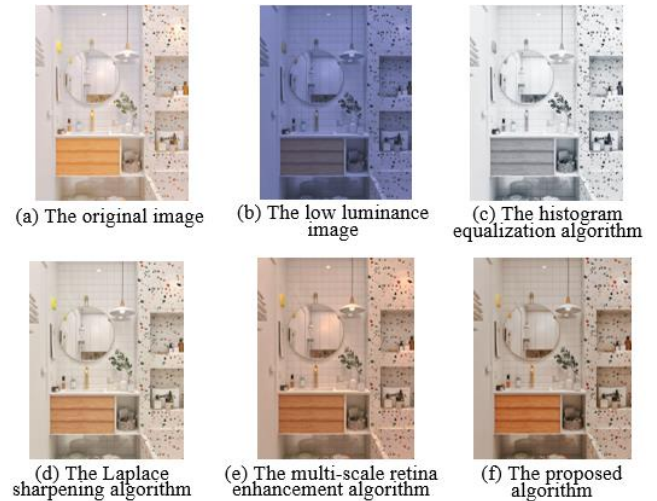

(a) The original image (b) The low luminance image (c) The histogram equalization algorithm

(d) The Laplace sharpening algorithm (e) The multi-scale retina enhancement algorithm (f) The proposed algorithm

Figure 6. Comparative experiment of color image enhancement

The main reason is that the proposed algorithm can keep a low error and a high signal-to-noise ratio when processing images containing high-level noise. In contrast, other algorithms gave increased error and reduced image quality when processing such images. Compared with the Laplace sharpening algorithm and the multi-scale retina enhancement algorithm, the proposed algorithm had better preserved the information details of images, so that the visual effect of enhanced images is closer to the real scenes.

Table 4. The *SSIM* value of different methods in case of original image added with different-ratio Gaussian noise

Ratio of Gaussian Noise	5%, 10%, 15%	20%, 30%, 25%	50%, 45%, 30%	60%, 50%, 40%	55%, 65%, 50%
Average noise ratio	0.91	0.87	0.79	0.68	0.62
Non-local mean algorithm	0.91	0.82	0.63	0.57	0.52
Bilateral filter algorithm	0.92	0.82	0.66	0.61	0.56
Wave beam transform algorithm	0.91	0.84	0.68	0.61	0.57
The proposed model	0.95	0.93	0.87	0.76	0.74

Table 5. Comparison of subjective evaluation indicators of different enhancement algorithms

Algorithm	Indicator	Original Image 1	Original Image 2	Original Image 3	Original Image 4	Original Image 5
The Laplace sharpening algorithm	*MSE*	438.212	2313.2	4612.1	4913.1	1123.4
	PSNR	22.3414	14.3231	11.3214	11.2389	17.2313
	Computation time	1.32*s*	1.22*s*	1.32*s*	1.22*s*	1.43*s*
The multi-scale retina enhancement algorithm	*MSE*	423.313	2341.2	4513.4	4823.1	1175.2
	PSNR	22.4133	14.3213	11.5671	11.2411	17.2311
	Computation time	1.62*s*	1.62*s*	1.38*s*	1.47*s*	1.41*s*
The proposed algorithm	*MSE*	0.1312	0.0313	0.0231	0.0414	0.0315
	PSNR	62.3123	61.2313	61.234	62.9871	58.3678
	Computation time	2.96*s*	3.2*s*	3.01*s*	2.96*s*	3.01*s*

5. CONCLUSION

This study investigated a few color image processing methods, including noise removal and image enhancement, and the method proposed in this study exhibited powerful performance and obvious advantages in various experiments and evaluations.

In terms of denoising algorithms, the model proposed in this study gave high *PSNR* and *SSIM* values under different ratios of Gaussian noise, showing its excellent performance in preserving image details and good overall visual quality. In addition, compared with other algorithms, in case of increased ratio of Gaussian noise, the decrement of *PSNR* and *SSIM* of the proposed model was smaller, showing higher robustness.

In terms of image enhancement algorithms, the method proposed in this study also showed obvious advantages in retaining image details and colors and processing high-level noise, and attained very good results. In the meantime, the proposed method also showed excellent adaptivity and can be customized according to the specific characteristics of the image.

In terms of image restoration, the proposed method gave low relative error and high *PSNR* and *SSIM* when dealing with sparse noise of different levels. Especially in case of high-level sparse noise, the proposed method still kept low relative error and high *PSNR* and *SSIM*, demonstrating its good ability in dealing with complex situations.

In summary, regardless of qualitative visual effect or quantitative evaluation metrics, the proposed image processing method had outperformed other reference algorithms. So it has a great potential to be applied in more fields, such as medical image processing, remote sensing image analysis, and computer vision.

REFERENCES

[1] Hosono, K., Ono, S., Miyata, T. (2019). Weighted tensor nuclear norm minimization for color image restoration. IEEE Access, 7: 88768-88776. https://doi.org/10.1109/ACCESS.2019.2926507

[2] Zhu, Y.B. (2020). Color management of digital media art images based on image processing. Ingénierie des Systèmes d'Information, 25(4): 445-452. https://doi.org/10.18280/isi.250406

[3] Kumar, H.B.B., Chennamma, H.R. (2021). Classification of computer graphic images and photographic images based on fusion of color and texture features. Revue d'Intelligence Artificielle, 35(3): 201-207. https://doi.org/10.18280/ria.350303

[4] Palai, C., Jena, P.K., Khuntia, B., Mishra, T.K., Pattanaik, S.R. (2023). Content-based image retrieval using adaptive CIE color feature fusion. Revue d'Intelligence Artificielle, 37(1): 63-72. https://doi.org/10.18280/ria.370109

[5] He, Z., Tang, K., Fang, L. (2017). Cross-scale color image restoration under high density Salt-and-Pepper Noise. In 2017 IEEE International Conference on Image Processing (ICIP), Beijing, China, pp. 3780-3784. https://doi.org/10.1109/ICIP.2017.8296989

[6] Liu, X., Tang, G. (2023). Color image restoration using sub-image based low-rank tensor completion. Sensors, 23(3): 1706. https://doi.org/10.3390/s23031706

[7] Huang, C., Ng, M.K., Wu, T., Zeng, T. (2021). Quaternion-based dictionary learning and saturation-value total variation regularization for color image restoration. IEEE Transactions on Multimedia, 24: 3769-3781. https://doi.org/10.1109/TMM.2021.3107162

[8] Wang, W., Song, Q. (2022). Color image restoration based on saturation-value total variation plus L1 fidelity. Inverse Problems, 38(8): 085009. https://doi.org/10.1088/1361-6420/ac7a2b

[9] Vankayalapati, R., Muddana, A.L. (2021). Denoising of images using deep convolutional autoencoders for brain tumor classification. Revue d'Intelligence Artificielle, 35(6): 489-496. https://doi.org/10.18280/ria.350607

[10] Zeng, Y., Yi, W., Wang, Y., Wang, Q. (2022). A remote sensing image processing method based on color restoration and enhancement. In Thirteenth International Conference on Graphics and Image Processing (ICGIP 2021), 12083: 603-608. https://doi.org/10.1117/12.2623543

[11] Li, H., He, X., Bai, Y., Gong, F., Wang, D., Li, T. (2022). Restoration of wintertime ocean color remote sensing products for the high-latitude oceans of the southern hemisphere. IEEE Transactions on Geoscience and Remote Sensing, 60: 1-12. https://doi.org/10.1109/TGRS.2022.3228961

[12] He, Y., Li, C., Li, X. (2023). Remote sensing image dehazing using heterogeneous atmospheric light prior. IEEE Access, 11: 18805-18820. https://doi.org/10.1109/ACCESS.2023.3247967

[13] Hao, P., Ai, D., Zang, L., Fan, J., Yang, J. (2022). Color restoration method for endoscope image using multiscale discriminator based model compression strategy. In 2022 7th International Conference on Computational Intelligence and Applications (ICCIA), Nanjing, China, pp. 161-166. https://doi.org/10.1109/ICCIA55271.2022.9828438

[14] Rehman, A., Butt, M.A., Zaman, M. (2022). Liver lesion segmentation using deep learning models. Acadlore Transactions on AI and Machine Learning, 1(1): 61-67. https://doi.org/10.56578/ataiml010108

[15] Liu, C. H., Yang, J. H., Liu, Y., Zhang, Y., Liu, S., Chaikovska, T., Liu, C. (2023). Artificial intelligence in cervical cancer research and applications. Acadlore Transactions on AI and Machine Learning, 2(2): 99-115. https://doi.org/10.56578/ataiml020205

[16] Panetta, K., Shreyas Kamath, S.K., Rao, S.P., Agaian, S.S. (2022). Deep perceptual image enhancement network for exposure restoration. IEEE Transactions on Cybernetics, 53(7): 4718-4731. https://doi.org/10.1109/TCYB.2021.3140202

[17] Al-Otum, H.M., Ellubani, A.A.A. (2022). Secure and effective color image tampering detection and self restoration using a dual watermarking approach ☆. Optik, 262: 169280.

https://doi.org/10.1016/j.ijleo.2022.169280

[18] Zhang, L.M., Chao, W.W., Liu, Z.Y., Cong, Y., Wang, Z.Q. (2022). Crack propagation characteristics during progressive failure of circular tunnels and the early warning thereof based on multi-sensor data fusion. Geomechanics and Geophysics for Geo-Energy and Geo-Resources, 8: 172. https://doi.org/10.1007/s40948-022-00482-3

[19] Zhang, L.M., Wang, X.S., Cong, Y., Wang, Z.Q., Liu, J. (2023). Transfer mechanism and criteria for static–dynamic failure of granite under true triaxial unloading test. Geomechanics and Geophysics for Geo-Energy and Geo-Resources, 9: 104. https://doi.org/10.1007/s40948-023-00645-w

[20] Wang, S., Sun, Y. (2022). Image extraction of mural line drawing based on color image segmentation algorithm. In CIPA 2022: Proceedings of the 2nd International Conference on Cognitive Based Information Processing and Applications, Changzhou, China, pp. 55-62. https://doi.org/10.1007/978-981-19-9376-3_7

[21] Liu, X., Tang, G. (2023). Color image restoration using sub-image based low-rank tensor completion. Sensors, 23(3): 1706. https://doi.org/10.3390/s23031706

[22] Huang, Y., Yuan, F., Xiao, F., Cheng, E. (2022). Underwater image enhancement based on color restoration and dual image wavelet fusion. Signal Processing: Image Communication, 107: 116797. https://doi.org/10.1016/j.image.2022.116797

[23] Zhou, J., Wei, X., Shi, J., Chu, W., Lin, Y. (2022). Underwater image enhancement via two-level wavelet decomposition maximum brightness color restoration and edge refinement histogram stretching. Optics Express, 30(10): 17290-17306. https://doi.org/10.1364/OE.450858

[24] Li, T., Rong, S., Zhao, W., Chen, L., Liu, Y., Zhou, H., He, B. (2022). Underwater image enhancement using adaptive color restoration and dehazing. Optics Express, 30(4): 6216-6235. https://doi.org/10.1364/OE.449930

[25] Meng, H., Yan, Y., Cai, C., Qiao, R., Wang, F. (2020). A hybrid algorithm for underwater image restoration based on color correction and image sharpening. Multimedia Systems, 28: 1975-1985. https://doi.org/10.1007/s00530-020-00693-2